This article has been accepted for publication in a future issue of this journal, but has not been fully edited. Content may change prior to final publication. Citation information: DOI 10.1109/TII.2016.2586461, IEEE Transactions on Industrial Informatics

Enhanced Flicker Mitigation In DFIG-Based Distributed Generation of Wind Power

Moataz Ammar, *Member, IEEE,* and Mohammed E. Ammar, *Member, IEEE*

***Abstract*—Upon the connection of wind generators (WGs) to distribution grids, significant flicker emission can appear, due to the low X/R ratios and low short-circuit levels at the points of connection. This paper proposes a reactive-power-based control scheme that aims for accurate cancellation of voltage flicker resulting from the grid connection of DFIG-based wind power. The control scheme operation is based on constructing the two-bus equivalent network of the detailed power system, via local measurements of voltage and active and reactive power flows at the DFIG terminals. The reactive power flow at the DFIG terminals is adjusted accordingly to cancel voltage flicker, based on the constructed equivalent network equations. The proposed control scheme avoids the use of power flow approximations at the connection point, and hence is free of the inaccuracies implicated in the conventional reactive-power-based flicker mitigation approaches (based on power factor control and voltage control). The proposed control scheme is shown, by comparative results, to provide superior performance to those conventional flicker mitigation approaches, as well as flicker mitigation capability independent of the connection point parameters.**

***Index Terms*—DFIG, distributed generation, flicker, power quality, reactive power control, wind power.**

I. Introduction

FLICKER emission is a power quality concern associated with the integration of wind generators (WGs) to the power system, in general [1], and distribution networks in particular, due to their inherent flicker susceptibility [2], [3]. Based on the nature of loads connected to a distribution network, the flicker emission limit allocated to a prospective distributed generation (DG) project is determined [4], [5]. This results in either limiting the capacity of the WGs to be connected "fit-and-forget approach" [6], [7] or necessitating the presence of flicker mitigation controls or equipment to allay the severity of the flicker emission. A flicker mitigation control scheme can be either based on reactive power control or active power control [8], [9]. Reactive power control for flicker mitigation purposes was investigated in depth in [8], [10], [11]. The works in [8], [10] outlined the ability of leading power factor operation of the DFIG in reducing its flicker emission. While the work in [11] studied the operational limitations of such approach and voltage control in distribution networks. Those two approaches have significant limitations in distribution networks, as they are highly dependent on the network X/R ratio and require the DFIG to absorb significant amounts of reactive power. Such amounts of reactive power are beyond the DFIG capabilities [12], [13], and are restricted by the operative grid codes [14]. In order to overcome those limitations, the work in [11] proposed the operation of the DFIG at a variable power factor. This was realized by compensating the flicker-producing and the non-flicker-producing active power changes of the WG separately, resulting in more flexibility with the WG recative power behavior and decreased consumption of reactive power. Both leading power factor and variable power factor control modes were shown to have their flicker mitigation capability decrease as the size of wind power at the connection point increases [15]. This is a result of the inability to characterize/control the voltage changes at the connection point based on the distribution network X/R ratio, as assumed to hold.

Active power smoothing as a flicker mitigation approach was proposed in [9], [16], [17], [15] to overcome the above mentioned limitations. Particularly, the work in [9] proposed the modification of the control scheme of the DC-link of the full-converter synchronous WG to act as a storage unit to store a portion of the wind power flicker-producing fluctuations. While the work in [16] proposed a modification to the pitch control algorithm of the DFIG to alleviate its flicker emission. The use of a dedicated energy storage system (ESS) to smooth the WG flicker-producing fluctuations was proposed in [17], [15]. In [17], a controller was proposed for a flywheel-based ESS to offset the 3p torque oscillations of WGs. In [15], a supercapacitor-based dedicated ESS was proposed to smooth the entire spectrum of WGs flicker-producing fluctuations. The cited works have shown that all the above mentioned approaches demonstrate a level of flicker mitigation. Yet, those approaches are however associated with certain concerns and shortcomings. On one hand, the limitation of the reactive-power-based flicker mitigation approaches is seen in approximations utilized at the connection point, and therefore the grid impedance and wind power rating dependence of those approaches [15]. When those approximations accuracy is impaired, they fail to properly characterize the voltage fluctuations at the connection point and consequently result in impaired flicker mitigation. On the other hand, the implementation of a dedicated ESS requires the deployment of external equipment and controls to a wind farm, which may constitute a financial burden on the DG project.

In light of those concerns, this paper proposes an enhanced reactive-power-based DFIG flicker mitigation control scheme, that is independent of the common approximations regarding distribution networks voltage fluctuations characterization, and is therefore suitable for any connection point parameters. The DFIG is of interest in this work due to its popularity as a WG

Moataz Ammar is with NextEra Energy Resources (e-mail: moataz.ammar@mail.mcgill.ca).

Mohammed E. Ammar is with the Department of Electric Power and Machines, Cairo University (e-mail: mohammed.ammar@eng.cu.edu.eg).

Copyright (c) 2009 IEEE. Personal use of this material is permitted. However, permission to use this material for any other purposes must be obtained from the IEEE by sending a request to pubs-permissions@ieee.org.

1551-3203 (c) 2016 IEEE. Personal use is permitted, but republication/redistribution requires IEEE permission. See http://www.ieee.org/publications_standards/publications/rights/index.html for more information.

This article has been accepted for publication in a future issue of this journal, but has not been fully edited. Content may change prior to final publication. Citation information: DOI 10.1109/TII.2016.2586461, IEEE Transactions on Industrial Informatics

topology [18], emanating from its reduced converter size, low-installation cost and wide speed range of operation [19], [20]. The proposed control scheme uses the active power, reactive power and voltage measurements at the DFIG terminals to mathematically calculate the required DFIG reactive power adjustment, such that the connection point voltage maintains its desired waveform (free of flicker content).

This paper is structured as follows: Section II introduces the power system and WG models employed in this work. Section III describes the limitations of the currently adopted reactive-power-based flicker mitigation approaches. Section IV describes the proposed flicker mitigation control scheme and its implementation. Section V provides simulation results, evaluation of the proposed control scheme and comparison with other flicker mitigation control options. Section VI encapsulates the conclusions of this body of work.

II. Power System and WG Models

A. Power System Model and Flicker Measurement

The power system with respect to wind power flicker emission is characterized by its short-circuit capacity ratio (SCR), and the network X/R ratio at the point of connection, as outlined in IEC standard 61400-21 [21]. The SCR is defined as the ratio of short-circuit level at the point of connection to the wind power rated capacity. Fig. 1 is the circuit model used in [21] to conduct WG flicker severity studies, and is used in this work to explain the conventional flicker mitigation approaches and carry out parametric studies. A distribution feeder is used to reflect the practical implementation of the proposed control scheme. The IEC flickermeter described in IEEE Standard 1453-2011 [22] is used for flicker measurement. The benchmark for flicker severity comparison in this work is the short-term flicker index P_{st}, and the flicker measurements are conducted based on the required 10-minute simulation time frame [22].

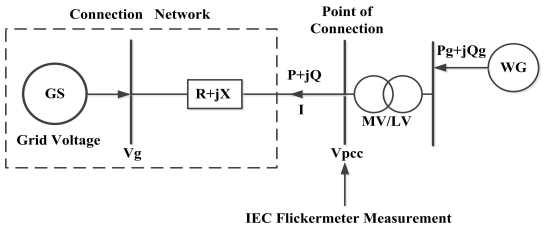

Fig. 1. Power system representation for WG flicker studies.

B. DFIG Structure and Control

The DFIG comprises two converters, a Grid-Side (GS) converter and a Rotor-Side (RS) converter. The converters control is achieved through decoupled dq control such that the active and reactive power delivered by the machine are controlled independently. The RS converter d-axis current control aims for maintaining an optimal rotational speed of the WG, while its q-axis current control aims for delivering a reference setting of reactive power from the RS converter. The GS converter control is achieved similarly by means of d-axis current control, aiming for a constant DC link capacitor voltage, and q-axis current control delivering a reference setting of reactive power from the GS converter. A WG reactive power setting is typically based on one of the conventional reactive power control approaches known in the industry [11], and in the DFIG can be delivered entirely by one of the converters or shared between the two converters [23]. Fig. 2 shows the control schematic of the DFIG model in use.

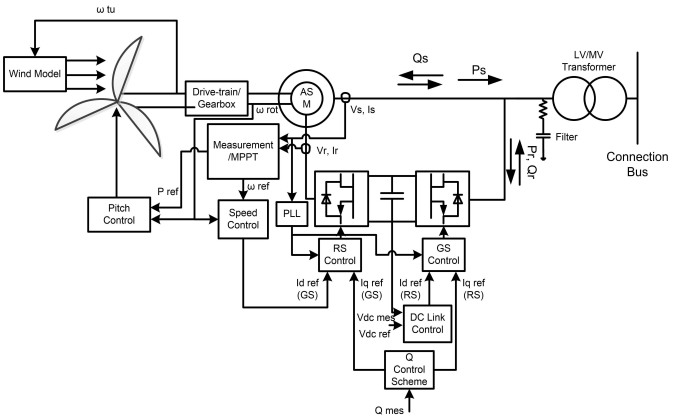

Fig. 2. DFIG control schematic.

C. Wind Turbine and Flicker Emission Modeling

A 10-minute wind speed time-series sampled at 0.1 s was used [11] and the aerodynamics at the turbine blades and the tower shadow effect were modeled based on the model suggested in [24]. The rotational speed of the turbine is coupled to the mathematical model of [24] for continuous update of the turbine speed impact on the frequency of the tower shadow, Fig. 2.

TABLE I
Generator Parameters

Parameter	Value	unit
Active power rating	2	MW
Rotor resistance	0.016	pu
Rotor inductance	0.16	pu
Stator resistance	0.023	pu
Stator inductance	0.18	pu
Generator inertia constant	0.8	s

TABLE II
Wind Turbine Parameters

Parameter	Value	unit
Hub height	90	m
Rotor radius	40	m
Tower radius	2	m
Distance from blade origin to tower midline	3	m
Wind shear exponent	0.3	–
Turbine inertia constant	4.2	s

1551-3203 (c) 2016 IEEE. Personal use is permitted, but republication/redistribution requires IEEE permission. See http://www.ieee.org/publications_standards/publications/rights/index.html for more information.

This article has been accepted for publication in a future issue of this journal, but has not been fully edited. Content may change prior to final publication. Citation information: DOI 10.1109/TII.2016.2586461, IEEE Transactions on Industrial Informatics

The parameters of the generator and wind turbine in use are shown respectively in Table. I and Table. II. The simulations are conducted in MATLAB Simulink.

With respect to the given parameters, the output power of the DFIG unit in use is shown in both its temporal and spectral forms in Fig. 3, for an average wind speed of 10 m/s and turbulence intensity of 15 %.

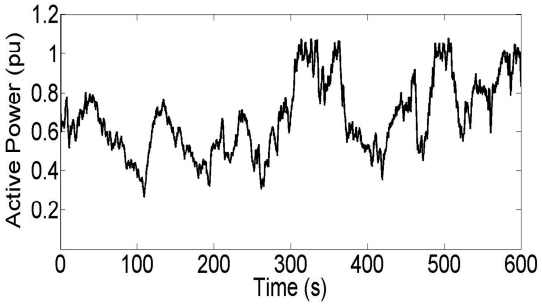

(a)

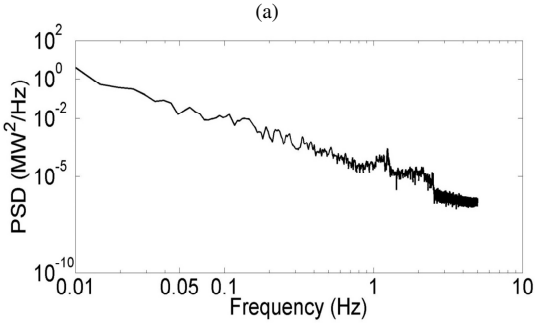

(b)

Fig. 3. Output power of the DFIG unit at an average wind speed of 10 m/s and turbulence intensity of 15 %: (a) ten-minute temporal plot, (b) corresponding power spectral density plot.

III. Limitation of Conventional Reactive Power Control in Flicker Mitigation

The reactive power control approaches used for WG flicker mitigation are based on assumptions about the WG connection point. Basically, the concept is to simplify (1) (in reference to Fig. 1) to reach an approximate formula that expresses the voltage changes at the connection point in terms of the active and reactive power flows, at the WG connection point, and as a function of the network X/R ratio.

$$\vec{V_{pcc}} = \vec{V_g} + \vec{I}(R + jX) \tag{1}$$

Where $\vec{V_{pcc}}$ is the voltage at the connection point or the Point of Common Coupling (PCC), $\vec{V_g}$ is the grid voltage, $\vec{I}$ is the current flowing from the WG into the network, R and X are the equivalent power system resistance and reactance at the connection point respectively.

Particularly, by expressing the line current $\vec{I}$ in terms of the apparent power at the PCC (active power flow P and reactive power flow Q) and considering $\vec{V_g}$ to be the reference voltage with angle 0° and $\vec{V_{pcc}}$ to have an angle δ, (2) is derived. By carrying out basic mathematical operations on (2) and applying trigonometric substitutions, (3) and (4) are reached.

$$V_{pcc}\cos\delta + jV_{pcc}\sin\delta - V_g = \frac{P - jQ}{V_{pcc}\cos\delta - jV_{pcc}\sin\delta}\,(R + jX) \tag{2}$$

$$(V_{pcc}\cos\delta)^2 + (V_{pcc}\sin\delta)^2 - V_g(V_{pcc}\cos\delta - jV_{pcc}\sin\delta) = (PR + QX) + j(PX - QR) \tag{3}$$

$$V_{pcc}^2 - V_gV_{pcc}\cos\delta + jV_gV_{pcc}\sin\delta = (PR + QX) + j(PX - QR) \tag{4}$$

A separation of the real and imaginary terms of (4) yields (5) and (6).

$$V_{pcc}^2 - V_gV_{pcc}\cos\delta = (PR + QX) \tag{5}$$

$$V_gV_{pcc}\sin\delta = (PX - QR) \tag{6}$$

The approximate voltage changes formula is reached by assuming that the angle δ approaches zero, and therefore (7) becomes a valid approximation of (5).

$$\Delta V = V_{pcc} - V_g \approx \frac{PR + QX}{V_{pcc}} \tag{7}$$

If (7) holds, any change in voltage magnitude at the WG connection point becomes controllable by the WG reactive power flow, as a function of the network X/R ratio. Yet, as the value of δ increases, (7) ceases to properly designate the voltage fluctuations at the connection point and the efficiency of a flicker mitigation scheme based on (7) is undermined [15]. The value of δ cannot be neglected for wind power integration at low $SCRs$, which situations are the most susceptible to the DG flicker problem [25]. The value of δ increases by the increase of wind power capacity at the connection point (decrease of SCR) and further increases by the operation of the WGs at a leading power factor (as required for flicker mitigation). Particularly, Fig. 4 demonstrates the flicker mitigation feasibility based on (7). P_{st} values are shown for three interconnection scenarios (three $SCRs$ at an X/R ratio of 2), for cases with and without flicker mitigation based on power factor control. This range of $SCRs$ is typical of those observed in flicker-susceptible DG connection points, shown in [25].

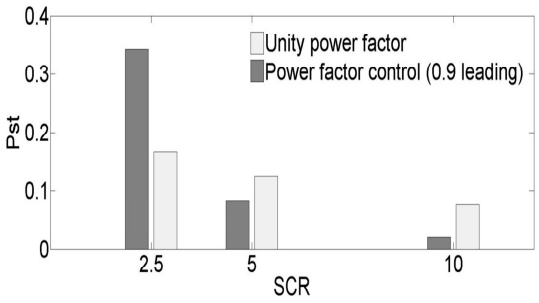

Fig. 4. Pst values vs. SCR under operation at a leading power factor at an X/R of 2, average wind speed of 10 m/s and turbulence intensity of 15 %.

1551-3203 (c) 2016 IEEE. Personal use is permitted, but republication/redistribution requires IEEE permission. See http://www.ieee.org/publications_standards/publications/rights/index.html for more information.

This article has been accepted for publication in a future issue of this journal, but has not been fully edited. Content may change prior to final publication. Citation information: DOI 10.1109/TII.2016.2586461, IEEE Transactions on Industrial Informatics

It can be seen from Fig. 4 that flicker mitigation by leading power factor control, based on (7), fails to achieve its goals as the SCR decreases. On the contrary, it aggravates the flicker emission as (7) ceases to properly describe the voltage changes at the connection point. The implementation of closed-loop voltage control is likely to have an improved performance due to its feedback feature, but implies an undesired control mode in DG [26], and is still liable to power flow approximations. Consequently, a more encompassing flicker mitigation control scheme is desired. In the following section, the proposed control scheme is presented. The advantages of the proposed control scheme, in comparison to existing flicker mitigation schemes, can be summarized in the following points: 1)-the feasibility of flicker mitigation independent of the X/R ratio and SCR at the point of connection, as opposed to the methods in [8], [11], 2)-higher flicker mitigation than existing reactive-power-based methods [8], [10], [11], due to improved estimation of the reactive power quantity required to mitigate flicker, 3)-no need for external equipment (energy storage) or significant control changes (pitch control changes) within the WG, as required in [15], [16], 4)-maintains the WG ability to function as a sink or a source of reactive power, as required in utilities grid codes [14].

IV. Proposed Flicker Mitigation Control Scheme

A. Methodology

The central premise of the proposed control scheme is that a value always exists for the reactive power flow Q, at the WG terminals, that when achieved by the WG converters, the voltage impacts of the WG flicker-producing P fluctuations will vanish. This value is thereafter referred to as Q_{ref}. The proposed control scheme uses the measurements available at the WG terminals and the given connection point parameters to find Q_{ref}, through the construction of the power system rudimentary two-bus equivalent network. Particularly, constructing such network (depicted in Fig. 5) requires the availability of the following: 1)-the X and R values at the connection point (given parameters), 2)-the P, Q and V_{pcc} values (available measurements to the WG), and 3)-the connection point open-circuit voltage V_g (can be calculated by means of the measured variables).

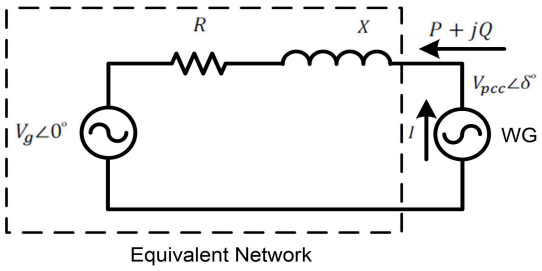

Fig. 5. Two-bus equivalent network at the WG point of connection.

Particularly, the acquisition of Q_{ref} can be decomposed in the following stages:

1) Obtaining a Q expression: To find Q_{ref}, some mathematical operations are required to find a Q expression as a function of the Fig. 5 network parameters. Namely, by moving V_{pcc}^2 to the right-hand side of (5), then squaring both sides of (5) and (6), (8) can be obtained and after rearrangement can be written as (9).

$$V_{pcc}^4 - 2PRV_{pcc}^2 - 2QXV_{pcc}^2 + (PR)^2 + (PX)^2 + (QR)^2 + (QX)^2 = V_{pcc}^2 V_g^2 \tag{8}$$

$$Q^2 - Q(\frac{2XV_{pcc}^2}{R^2+X^2}) - (\frac{V_{pcc}^2 V_g^2 - (PR)^2 - (PX)^2 - V_{pcc}^4 + 2PRV_{pcc}^2}{R^2+X^2}) = 0 \tag{9}$$

Equation (9) is an expression of Q that can be solved at the sought value of V_{pcc} (V_{pcc} value free of the WG flicker-producing P fluctuations impact).

2) Obtaining V_g: The value of δ can be written as an expression of the WG available measurements, (10) (the combination of (5) and (6)). The value of V_g can then be calculated by evaluating (6) with δ substituted for in terms of the WG available measurements, as shown in (11).

$$tan(\delta) = -\frac{PX - QR}{PR + QX - V_{pcc}^2} \tag{10}$$

$$V_g = \frac{PX - QR}{V_{pcc}\sin\left(\arctan\left(-\frac{PX-QR}{PR+QX-V_{pcc}^2}\right)\right)} \tag{11}$$

3) Obtaining Q_{ref}: As stated earlier, Q_{ref} is an amount of reactive power flow at the WG terminals, that cancels the effect of the WG flicker-producing P fluctuations. The flicker-producing P fluctuations are those occurring at a repetition rate of above 0.05 Hz [22]. Therefore, if a low-pass-filtered measurement of V_{pcc}, V_{pcc-lp} (filtered with a cut-off frequency of 0.05 Hz), is used to solve (9) for a Q value, at the calculated V_g and the measured P, Q_{ref} is obtained. Solving (9) at V_{pcc-lp} means that the changes in P accounting for the flicker emission will be counteracted by the continuously updated Q_{ref} to maintain (V_{pcc-lp}), (12).

Let

$b = (\frac{2XV_{pcc-lp}^2}{R^2+X^2})$,

$c = (\frac{V_{pcc-lp}^2 V_g^2 - (PR)^2 - (PX)^2 - V_{pcc-lp}^4 + 2PRV_{pcc-lp}^2}{R^2+X^2})$,

$$Q_{ref} = \frac{-b \pm \sqrt{b^2 - 4c}}{2} \tag{12}$$

Q_{ref} is an exact solution that cancels voltage flicker at the WG terminals. Q_{ref} obtained from (12) has two solutions. Due to the significance of the term b^2 with respect to $4c$, $\sqrt{b^2-4c}$ approaches b, and the Q_{ref} solution of the higher magnitude is several multiples of the solution of the lower magnitude and occurs outside the range of the WG operation limits. The lower magnitude of Q_{ref} is applied. Lower machine currents and losses are also a reason for choice of the lower magnitude value. A complex Q_{ref} solution is implicitly avoided in the

1551-3203 (c) 2016 IEEE. Personal use is permitted, but republication/redistribution requires IEEE permission. See http://www.ieee.org/publications_standards/publications/rights/index.html for more information.

This article has been accepted for publication in a future issue of this journal, but has not been fully edited. Content may change prior to final publication. Citation information: DOI 10.1109/TII.2016.2586461, IEEE Transactions on Industrial Informatics

planning phase of a MV-connected DG project, where the connection is made to MV networks composed of resistances and reactances and voltage magnitudes controllable by reactive power changes. A complex Q_{ref} solution implies the necessity of additional active power control to achieve the desired voltage control. This situation is of concern in LV networks with highly resistive conductors.

B. Control Scheme Realization in the DFIG

A WG is typically required to be capable to absorb or inject a utility-specified amount of reactive power, in case it is required to function as a source or a sink of reactive power. Therefore, Q_{ref} can be solely a flicker-mitigating quantity, if no reactive power requirement is placed on the WG, or can be a utility-specified amount of reactive power on which a flicker-mitigating quantity is superimposed.

In the proposed control scheme, the GS converter is dedicated for any utility-specified reactive power requirement Q_{GS}, and the flicker-mitigating quantity is assigned to the RS converter Q_{RS}. The separation of the flicker-mitigating quantity Q_{RS} from Q_{ref} can be achieved by deducting the low-pass-filtered Q flow Q_{lp} from Q_{ref}. Q_{lp} corresponds to the magnitude of the voltage level V_{pcc-lp} and also includes any reactive power contribution from the DFIG switching harmonics filter. In essence, the proposed control scheme confines V_{pcc} to a low-frequency spectrum of changes.

The flicker control scheme realization in the DFIG is shown in Fig. 6. Fig. 6 depicts the proposed RS (Fig. 6 (a)) and GS (Fig. 6 (b)) reactive power controls. The GS converter adheres to the typical desired power factor control operation, by maintaining the WG phase angle ϕ at a desired value, and the RS converter adjusts the reactive power around that value to cancel flicker, based on (12).

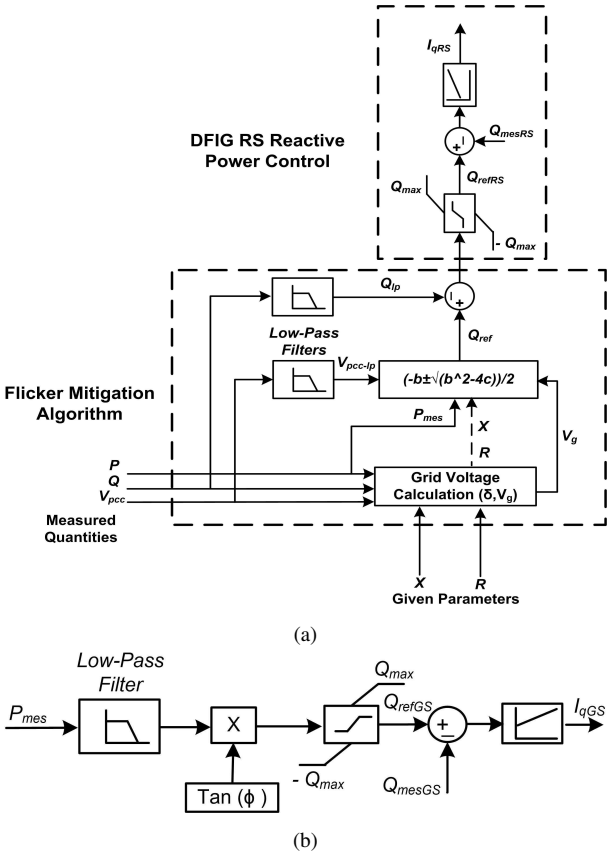

Fig. 6. Flicker mitigation control scheme: (a) RS reactive power control, (b) GS reactive power control.

C. Control Algorithm Summary

The flicker control algorithm can be summarized in the following steps:

1) Read the power system impedance at the point of connection, and the utility required reactive power demand Q_{GS} (delivered by the GS converter).
2) Measure P, Q and V_{pcc} at the WG terminals and obtain the value of V_g using (11).
3) Solve for a value of Q that maintains V_{pcc} at its low-pass-filtered measurement as P changes (plugging V_g, P and V_{pcc-lp} in (12) to obtain Q_{ref}).
4) Deduct the value of Q_{lp} from Q_{ref} and specify Q_{RS} to mitigate flicker by the RS converter.
5) Reiterate steps 2 through 5.

V. Study Cases and Simulation Results

In order to demonstrate the effectiveness of the proposed control scheme, several case studies have been investigated and under different operating conditions of the DFIG. The following cases were studied for the corresponding purposes below:

1) Variation of the average wind speed and turbulence intensity at the installation site: for demonstration of the proposed control scheme effectiveness for different site conditions (zero reactive power reference for the GS converter and network model as per [21]).
2) Variation of the connection point characteristics, in terms of the X/R ratio and SCR: for demonstration of the proposed control scheme effectiveness for different connection point characteristics (zero reactive power reference for the GS converter and network model as per [21]).
3) A 5-bus detailed distribution feeder with a connected wind farm capacity of 6 MW (3 DFIG units): for demonstration of the ability of the proposed control scheme to simultaneously control the flicker severity and the voltage level at the wind farm bus of connection (flicker mitigation with zero, positive and negative GS converter reactive power references); and for demonstration of the superior performance of the proposed control scheme, in comparison to the conventional flicker mitigation approaches (leading power factor and voltage control).

A. Effectiveness for Different Site Conditions

The turbulence intensity and the average wind speed at the WG turbine blades were changed and the flicker severity was observed, while maintaining the same connection point characteristics. The results are shown in Fig. 7 and Fig. 8 respectively. Fig. 7 shows that the P_{st} values changed from 0.12 at 10 % turbulence intensity to 0.19 at a turbulence

1551-3203 (c) 2016 IEEE. Personal use is permitted, but republication/redistribution requires IEEE permission. See http://www.ieee.org/publications_standards/publications/rights/index.html for more information.

This article has been accepted for publication in a future issue of this journal, but has not been fully edited. Content may change prior to final publication. Citation information: DOI 10.1109/TII.2016.2586461, IEEE Transactions on Industrial Informatics

intensity of 20 % (wind speed of 10 m/s). The corresponding P_{st} values under the proposed control scheme changed from 0.03 to 0.05. Similarly, Fig. 8 shows that the P_{st} values changed from 0.12, at an average wind speed of 8 m/s, to 0.19 at an average wind speed of 12 m/s (turbulence intensity of 15 %). The corresponding P_{st} values under the proposed control scheme changed from 0.029 to 0.049. The proposed control scheme remained effective in all cases.

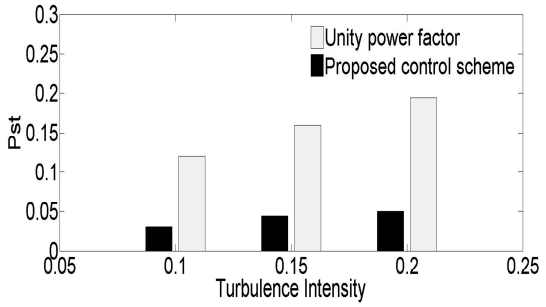

Fig. 7. Pst values vs. turbulence intensity at an average wind speed of 10 m/s, X/R ratio of 2 and SCR of 3.

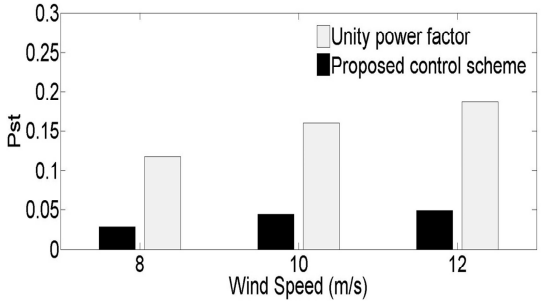

Fig. 8. Pst values vs. average wind speed at a turbulence intensity of 15 %, X/R ratio of 2 and SCR of 3.

B. Effectiveness for Different Connection Point Characteristics

A range of $SCRs$ was tested under three conditions: the DFIG operation without flicker mitigation; with flicker mitigation based on power factor control, (0.9 leading) based on (7); and with the proposed control scheme. The results are shown in Fig. 9. Fig. 9 shows that the proposed control scheme provides flicker mitigation irrespective of the SCR at which the WG connection is made. It is also seen that by comparison to flicker mitigation based on power factor control, the proposed control scheme always provides superior flicker mitigation. Moreover, it is seen that as the SCR decreases, the power factor control approach, and as outlined in previous sections, loses its flicker mitigation capability. Similarly, the performance with respect to the network X/R ratio is shown in Fig. 10. Fig. 10 shows that the proposed control scheme effectiveness is independent of the network X/R ratio.

C. 5-Bus distribution feeder

A distribution feeder consisting of 4 sections of a weak MV conductor of an X/R ratio of 1 is employed. The total feeder

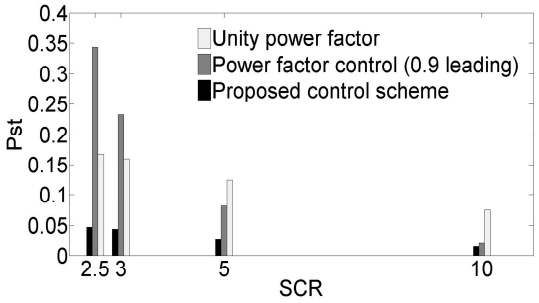

Fig. 9. Pst values vs. SCR under the proposed control scheme at an X/R ratio of 2, average wind speed of 10 m/s and turbulence intensity of 15 %.

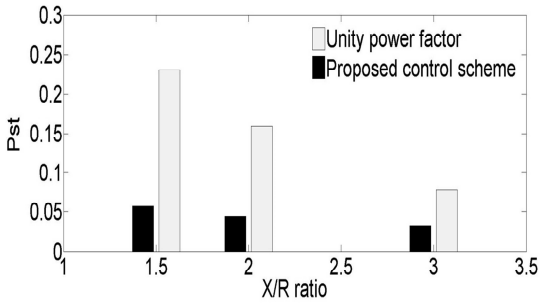

Fig. 10. Pst values vs. X/R ratio under the proposed control scheme at an SCR of 3, average wind speed of 10 m/s and turbulence intensity of 15 %.

loading is 10 MW and 2.5 MVAR. The HV/MV transformer is of 15 MVA and X/R ratio of 10 and the MV/LV transformers at the WGs side are each of 2.5 MVA and X/R ratio of 10. Bus 5 is the wind farm connection point. The specifics of Bus 5 as a connection point for the connected 6 MW wind farm (3 2 MW DFIG units) are: a short-circuit level of 23 MVA, X/R ratio of 1.1, SCR of 3.8, $R = 16.24\,\Omega$, and $X = 17.9\,\Omega$. The feeder layout is shown in Fig. 11.

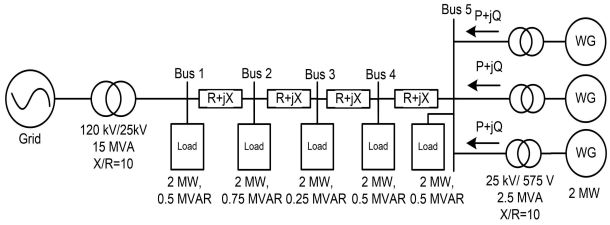

Fig. 11. Distribution feeder layout.

The performance of the proposed control scheme was evaluated by conducting the following two sets of tests: *Set 1*-testing of the proposed control scheme efficiency for different requirements on the GS converters reactive power reference, and *Set 2*-comparison of the efficiency of the proposed control scheme with the conventional flicker mitigation approaches (leading power factor and voltage control).

The first set of tests, *Set 1*, was conducted by observing the reactive power consumption of the DFIGs converters and the P_{st} values for the following three cases: Case 1, the operation under the proposed control scheme with zero reactive power

1551-3203 (c) 2016 IEEE. Personal use is permitted, but republication/redistribution requires IEEE permission. See http://www.ieee.org/publications_standards/publications/rights/index.html for more information.

This article has been accepted for publication in a future issue of this journal, but has not been fully edited. Content may change prior to final publication. Citation information: DOI 10.1109/TII.2016.2586461, IEEE Transactions on Industrial Informatics

reference to the GS converters; Case 2, the operation under the proposed control scheme with 0.97 leading power factor reactive power reference to the GS converters; and Case 3, the operation under the proposed control scheme with 0.97 lagging power factor reactive power reference to the GS converters. The active power generation of the wind farm and the reactive power delivered by the DFIGs converters for the three cases are shown in Fig. 12. The smoothed Bus 5 RMS voltage waveforms corresponding to the above studied cases are shown in Fig. 13.

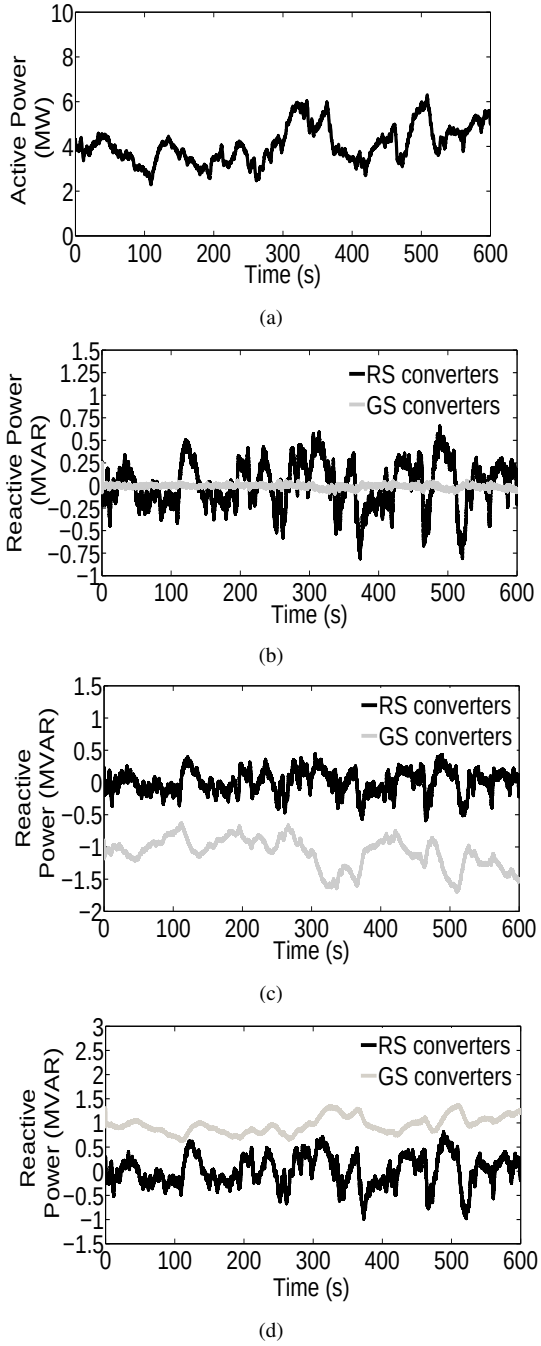

Fig. 12. Wind farm DFIGs active and reactive power flows (wind speed of 10 m/s and turbulence intensity of 10 %) : (a) wind farm active power generation, (b) wind farm reactive power consumption, Case 1, (c) wind farm reactive power consumption, Case 2, (d) wind farm reactive power consumption, Case 3.

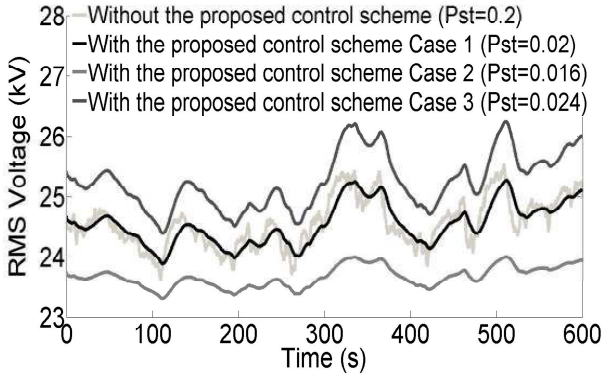

Fig. 13. RMS voltage at bus 5.

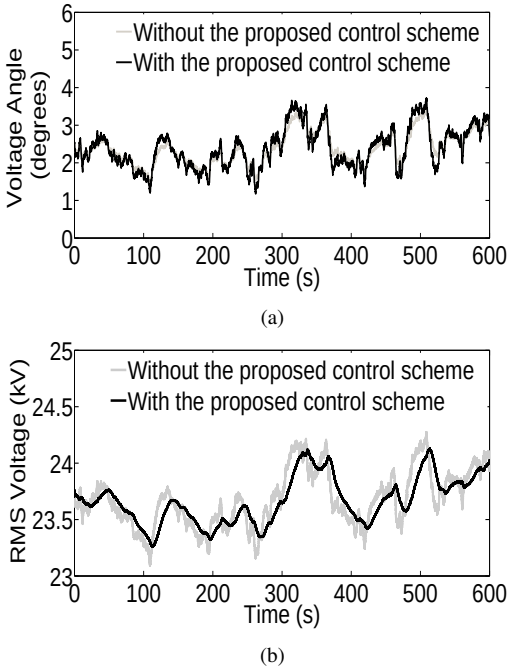

Fig. 14. Power system estimated parameters at bus 5, Case 1: (a) voltage angle δ, as estimated in one DFIG unit, (b) open-circuit voltage V_g, as estimated in one DFIG unit.

In Fig. 12 (b), the wind farm reactive power consumption in shown to be only administered by the DFIGs RS converters, solely responding to the voltage flicker concern, as outlined in the control scheme realization section. The resultant impact on the wind farm connection bus voltage is an alleviated flicker severity as aimed for, Fig. 13. The P_{st} value is reduced from a value of 0.2, without the proposed control scheme, to 0.02 with the proposed control scheme for this case (Case 1).

Conversely, in Fig. 12 (c), the wind farm reactive power consumption is shown to be administered by both the RS and the GS converters, responding to both the voltage flicker concern and a request on the wind farm to operate at a desired power factor (0.97 leading in that case). The resultant impact on the wind farm connection bus voltage is an alleviated flicker severity and a reduced magnitude of the connection bus RMS voltage, Fig. 13. The P_{st} value decreased from 0.2, without the proposed control scheme, to 0.016 with the

1551-3203 (c) 2016 IEEE. Personal use is permitted, but republication/redistribution requires IEEE permission. See http://www.ieee.org/publications_standards/publications/rights/index.html for more information.

This article has been accepted for publication in a future issue of this journal, but has not been fully edited. Content may change prior to final publication. Citation information: DOI 10.1109/TII.2016.2586461, IEEE Transactions on Industrial Informatics

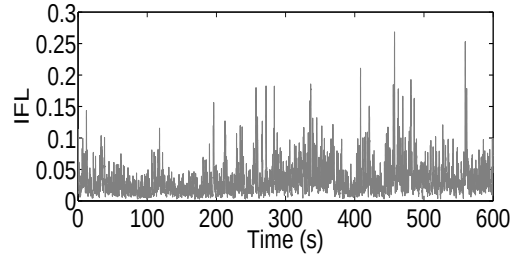

(a)

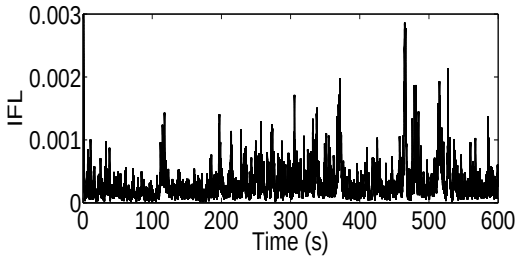

(b)

Fig. 15. Flickermeter IFL reading at bus 5: (a) without the proposed control scheme, (b) with the proposed control scheme, Case 1.

proposed control scheme for this case (Case 2). Similarly, in Fig. 12 (d), the reactive power is administered by both the RS and the GS converters, but with a request on the wind farm to operate at a 0.97 lagging power factor. The resultant impact on the wind farm connection bus voltage is an alleviated flicker severity and an increased magnitude of the connection bus RMS voltage, Fig. 13. The P_{st} value decreased from 0.2, without the proposed control scheme, to 0.024 with the proposed control scheme for this case (Case 3).

The voltage angle δ and the open-circuit voltage V_g as estimated in one of the DFIG units, for Case 1, are shown in Fig. 14. The instantaneous flicker level (IFL) reading detected by the IEC flickermeter, and from which the P_{st} index is calculated, is shown for completeness of illustration in Fig. 15, with and without the proposed control scheme, for Case 1.

The second set of tests, *Set 2*, was conducted by observing the flicker emission of the DFIGs under different flicker mitigation approaches. The test cases were conventional leading power factor control, within utility allowed limits (0.95 leading and 0.9 leading), and Bus 5 closed-loop voltage control by the DFIGs. The obtained P_{st} results are shown in Table. III.

TABLE III
COMPARISON OF FLICKER SEVERITY RESULTS (P_{st})

Approach	Unity Power Factor	Leading Power Factor (0.95)	Leading Power Factor (0.9)	Closed-Loop Voltage Control	Proposed Control Scheme (Case 1)
P_{st}	0.2	0.15	0.13	0.09	0.02

The results in Table. III show that the proposed control scheme provided 90 % decrease in P_{st}, in comparison to the original case in the absence of any flicker mitigation controls. The percentage P_{st} decrease under the application of closed-loop voltage control was 55 %, while the operation of the DFIGs at a leading power factor yielded a 35 % decrease in P_{st} at a leading power factor of 0.9 and a 25 % decrease at a leading power factor of 0.95. The proposed control scheme is seen to provide significant superiority in flicker mitigation when compared to the conventional flicker mitigation approaches.

It has to be noted that as the case is with all reactive-power-based flicker mitigation control schemes, the implementation of the proposed control scheme is subject to the flexibility of the imposed grid code with the reactive power capabilities of WGs. For instance, the proposed control scheme will not be applicable in case the operative grid code necessitates the operation of WGs or DG projects at a unity power factor. In such cases, flicker mitigation necessitates exercising control over the WG flicker-producing active power fluctuations.

VI. CONCLUSION

This paper proposed an enhanced flicker mitigation control scheme for the DFIG-based WGs. Rather than utilizing approximate voltage changes formulas at the connection point to achieve flicker mitigation, the proposed control scheme is based on online estimation of the variables of the detailed power system two-bus equivalent network. As a result, the proposed control scheme achieves accurate flicker mitigation independent of the SCR and the impedance X/R ratio at the WGs connection point. The proposed control scheme demonstrates superior performance to the conventional flicker mitigation approaches. The proposed control scheme was tested on the IEC standard 61400-21 test network and a 5-bus distribution feeder, of a weak wind farm connection point, and its effectiveness was shown to hold for a wide range of operating conditions.

REFERENCES

[1] L. Sheng-yen, W. Li, K. Shun-chin, and C. hao Chang, "Evaluation of measured power quality results of a wind farm connected to Taiwan power system," *IEEE Trans. on Ind. Appl.*, vol. 52, no. 1, pp. 42–49, Jan. – Feb. 2016.

[2] F. D. Kanellos and N. Hatziargyriou, "The effect of variable-speed wind turbines on the operation of weak distribution networks," *IEEE Trans. Energy Convers.*, vol. 17, no. 4, pp. 543–548, Dec. 2002.

[3] A. De Moura and A. De Moura, "Analysis of injected apparent power and flicker in a distribution network after wind power plant connection," *IET Renew. Power Gen.*, vol. 2, no. 2, pp. 113–122, Jun. 2008.

[4] "*Electromagnetic compatibility (EMC) - Part 3-7: Limits - Assessment of emission limits for the connection of fluctuating installations to MV, HV and EHV power systems*," IEC Standard 61000-3-7, 1996.

[5] M. Ammar, "Flicker emission of distributed wind power: A review of impacts, modeling, grid codes and mitigation techniques," in *IEEE Power and Energy Society General Meeting, 2012*, pp. 1–7.

[6] P. Siano, "Evaluating the impact of registered power zones incentive on wind systems integration in active distribution networks," *IEEE Trans. Ind. Informat.*, vol. 11, no. 2, pp. 523–530, Apr. 2015.

[7] M. Ammar, "A flicker allocation scheme for MV networks with high penetration of distributed generation," *IEEE Trans. on Power Del.*, vol. 31, no. 1, pp. 400–401, Feb. 2016.

[8] T. Sun, Z. Chen, and F. Blaabjerg, "Flicker study on variable speed wind turbines with doubly fed induction generators," *IEEE Trans. Energy Convers.*, vol. 20, no. 4, pp. 896–905, Dec. 2005.

1551-3203 (c) 2016 IEEE. Personal use is permitted, but republication/redistribution requires IEEE permission. See http://www.ieee.org/publications_standards/publications/rights/index.html for more information.

This article has been accepted for publication in a future issue of this journal, but has not been fully edited. Content may change prior to final publication. Citation information: DOI 10.1109/TII.2016.2586461, IEEE Transactions on Industrial Informatics

[9] W. Hu, Z. Chen, Y. Wang, and Z. Wang, "Flicker mitigation by active power control of variable-speed wind turbines with full-scale back-to-back power converters," *IEEE Trans. Energy Convers.*, vol. 24, no. 3, pp. 640–649, Sep. 2009.
[10] Y.-S. Kim and D.-J. Won, "Mitigation of the flicker level of a DFIG using power factor angle control," *IEEE Trans. Power Del.*, vol. 24, no. 4, pp. 2457–2458, Oct. 2009.
[11] M. Ammar and G. Joós, "Impact of distributed wind generators reactive power behavior on flicker severity," *IEEE Trans. Energy Convers.*, vol. 28, no. 2, pp. 425–433, Jun. 2013.
[12] M. Sujod, I. Erlich, and S. Engelhardt, "Improving the reactive power capability of the DFIG-based wind turbine during operation around the synchronous speed," *IEEE Trans. Energy Convers.*, vol. 28, no. 3, pp. 736–745, Sep. 2013.
[13] E. M. Y. C. K. Jinho Kim, Jul-Ki Seok, "Adaptive Q - V scheme for the voltage control of a DFIG-based wind power plant," *IEEE Trans. on Power. Electron.*, vol. 31, no. 5, pp. 3586–3599, May. 2016.
[14] "*Requirements for the Interconnection of Distributed Generation to the Hydro-Qubec Medium-Voltage Distribution System*," E.12-01, Montreal, 2009.
[15] M. Ammar and G. Joós, "A short-term energy storage system for voltage quality improvement in distrbuted wind power," *IEEE Trans. Energy Convers.*, vol. 28, no. 2, pp. 425–433, Dec. 2014.
[16] Y. Zhang, Z. Chen, W. Hu, and M. Cheng, "Flicker mitigation by individual pitch control of variable speed wind turbines with DFIG," *IEEE Trans. Energy Convers.*, vol. 29, no. 1, pp. 20–28, Mar. 2014.
[17] F. Diaz-Gonzalez, F. Bianchi, A. Sumper, and O. Gomis-Bellmunt, "Control of a flywheel energy storage system for power smoothing in wind power plants," *IEEE Trans. Energy Convers.*, vol. 29, no. 1, pp. 204–214, Mar. 2014.
[18] N. A. Orlando, M. Liserre, R. Mastromauro, and A. Dell'Aquila, "A survey of control issues in pmsg-based small wind-turbine systems," *IEEE Trans. Ind. Informat.*, vol. 9, no. 3, pp. 1211–1221, Aug. 2013.
[19] N. K. S. Naidu and B. Singh, "Doubly fed induction generator for wind energy conversion systems with integrated active filter capabilities," *IEEE Trans. Ind. Informat.*, vol. PP, no. 99, p. 1, Jun. 2015.
[20] J. Hu, J. Zhu, and D. Dorrell, "A new control method of cascaded brushless doubly fed induction generators using direct power control," *IEEE Trans. Energy Convers.*, vol. 29, no. 3, pp. 771–779, Sep. 2014.
[21] "*Wind turbines - Part 21: Measurement and assessment of power quality characteristics of grid connected wind turbines,*," IEC Standard 61400-21, 2008.
[22] "*IEEE Recommended Practice-Adoption of IEC 61000-4-15:2010 Electromagnetic Compatibility (EMC)-Testing and Measurement Techniques-Flickermeter-Functional and Design Specifications*," IEEE Standard 1453-2011, 2011.
[23] D. Zhou, F. Blaabjerg, T. Franke, M. Tonnes, and M. Lau, "Reduced cost of reactive power in doubly fed induction generator wind turbine system with optimized grid filter," *IEEE Trans. Power Electron.*, vol. 30, no. 10, pp. 5581–5590, Oct. 2015.
[24] D. S. Dolan and P. W. Lehn, "Simulation model of wind turbine 3p torque oscillations due to wind shear and tower shadow," *IEEE Trans. Energy Convers.*, vol. 21, no. 3, p. 717, Sep. 2006.
[25] A. Blavette, D. L. O'Sullivan, R. Alcorn, T. W. Lewis, and M. G. Egan, "Impact of a medium-size wave farm on grids of different strength levels," *IEEE Trans. Power Sys.*, vol. 29, no. 2, pp. 917–923, Mar. 2014.
[26] L. Tang, A. Yan, L. Marti, and J. Fuerth, "Hydro one distribution voltage performance design criteria and power distance test in enabling distributed generation," in *IEEE PES Transmission and Distribution Conference and Exposition (TD), 2012*, pp. 1–8.

Moataz Ammar (S'09-M'15) received the B.Eng. degree in electrical engineering from Cairo University, Giza, Egypt, the M.Sc.E. degree in electrical engineering from the University of New Brunswick, Fredericton, NB, Canada and the Ph.D degree in electrical engineering from McGill University, Montreal, QC, Canada.

His current research interests include grid interface of renewable energy sources, distributed generation, energy storage, power quality, and distribution system planning, operation and optimization.

M. E. Ammar (S'04-M'09) received the B.Sc. and M.Sc. degrees in electrical engineering from Cairo University, Cairo, Egypt in 2000 and 2003, respectively, and the Ph.D. degree in electrical engineering from the University of British Columbia, Vancouver, Canada in 2009. He was a postdoctoral research fellow at the University of British Columbia and a research associate at the University of Waterloo, Canada. From 2010-2012, he worked as a lead engineer for Invensys Operations Management. Currently, he is an assistant professor at Cairo University, Cairo, Egypt.

His research interests include control applications in power systems, distributed generation, renewable energy integration and smart grids.

1551-3203 (c) 2016 IEEE. Personal use is permitted, but republication/redistribution requires IEEE permission. See http://www.ieee.org/publications_standards/publications/rights/index.html for more information.